Applied Acoustics 104 (2016) 1–5

Contents lists available at ScienceDirect

Applied Acoustics

journal homepage: www.elsevier.com/locate/apacoust

Broadband resonant cavity inside a two-dimensional sonic crystal

Alejo Alberti [a], Pablo M. Gomez [b], Ignacio Spiousas [a], Manuel C. Eguia [a,*]

[a] Laboratorio de Acústica y Percepción Sonora, Universidad Nacional de Quilmes, R. S. Peña 352, Bernal, B1876BXD Buenos Aires, Argentina
[b] Laboratorio de Acústica y Electroacústica, Universidad de Buenos Aires, Av. Paseo Colón 850, C1063ACV Buenos Aires, Argentina

ARTICLE INFO

Article history:
Received 23 October 2014
Received in revised form 6 October 2015
Accepted 23 October 2015

Keywords:
Composite material
Band-gap
Broadband resonance

ABSTRACT

A rectangular cavity inside a two-dimensional sonic crystal was theoretically and experimentally characterized by examining its response to a cylindrical source emitting narrow-band filtered noise bursts with central frequencies ranging from 2 to 12 kHz. A broadband intensity resonance was observed for frequencies within the full band-gap region of the sonic crystal (5.5–6.5 kHz). Unlike ordinary resonances, this broadband resonance depends on the reflection properties of the sonic crystal forming the surrounding walls rather than on the geometry of the cavity.

1. Introduction

Recently, a great deal of effort has been devoted to the study of the transmission properties of periodic composite materials, such as sonic crystals. The existence of full band gaps [1], negative refraction [2], birefringence and negative birefringence [3] has been demonstrated for these systems, both experimentally and through theoretical calculations. Also, implementations of acoustic lenses [4], sound barriers [5], acoustic diodes [6,7], wide-band splitters [8] and acoustic switches [9] have been developed from periodic composite materials. These works evidence that sonic crystals are useful materials for controlling the propagation of sound. In contrast, the reflective properties of sonic crystals are less studied [10,11] and, with the exception of an acoustical antireflective coating [12,13], no applications have been yet proposed based on these properties. It has been shown that incident acoustic waves with frequencies within the band gap region are reflected back since their propagation inside the sonic crystal is inhibited [10], due to the destructive interference of scattered waves. This kind of reflection is observed both for full band gaps (inhibited propagation for all incidence angles), partial band gaps (inhibited propagation only for certain incidence angles) and deaf bands (propagation with energy transfer to higher Bragg modes).

In a previous work [14], it was proposed that these special reflective properties can be exploited to build a large (compared to the lattice parameter) cavity inside a sonic crystal. It was shown, through theoretical calculations, that this cavity possesses a particular structure of resonances that is more tied to the parameters of the sonic crystal lattice than to the geometry of the cavity itself. For example, the response of the cavity exhibits a broadband resonance for frequencies belonging to the full band gap region. In such a way, the sonic crystal cavity can be "tuned" by changing the lattice structure of the walls without changing the cavity dimensions, giving rise to new potential applications. Also, in contrast to previous works on sonic crystal defects obtained by removing a single element of the lattice [15], the dimensions of the cavity are large compared to the lattice parameter and the wavelength of the resonances.

In this work we will study the frequency response of a rectangular cavity inside a two-dimensional sonic crystal, as an experimental validation of the predicted broadband resonances. In [14] an approximation of the response of the cavity was made using a modified ray-tracing method, hence the results are valid only for a superposition of mutually incoherent components or narrow-band filtered noise. Here we will use this kind of stimulus to excite the sonic-crystal cavity. Also in this way we minimize the spatial inhomogeneities and the number of necessary measurement points for the characterization of the system.

2. Apparatus and methods

The experimental setup used in this paper is displayed in Fig. 1. The sample consisted of aluminum cylinders arranged in a 24×20 square matrix from which a central portion of 14×10 cylinders was removed to form a rectangular cavity surrounded by five rows thick sonic crystal "walls". The cavity was sandwiched between

* Corresponding author.
E-mail addresses: alejo.alberti@lapso.org (A. Alberti), pgomez@fi.uba.ar (P.M. Gomez), ispiousas@unq.edu.ar (I. Spiousas), meguia@unq.edu.ar (M.C. Eguia).

http://dx.doi.org/10.1016/j.apacoust.2015.10.022
0003-682X/

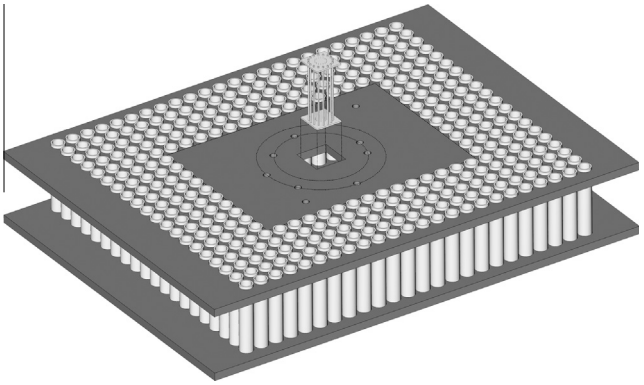

Fig. 1. Schematic representation of the experimental configuration of the sonic crystal cavity and the acoustic source (ionic transducer). The cavity is comprised by two hard plates covered with rubber (dark gray) and four sonic crystal "walls" formed by a square array of aluminum cylinders (light gray) of diameter 25.4 mm with a lattice parameter of 33 mm. The ionic transducer is inserted through the square hole at the center of the cavity and the nine measuring points are visible as holes drilled on the upper plate. The two dotted circles have radii of 8 and 11 cm.

two hard plates covered with rubber and separated 11 cm. The external diameter of the cylinders and the lattice constant were 25.4 and 33 mm respectively.

Since the sonic crystal and the cavity are idealized as two-dimensional, the sound source applied had to be cylindrical. Thus, we employed a custom-made ionic acoustic transducer built upon sixteen thin (100 μm) copper wires (corona electrodes) and the same number of 3 mm diameter brass rods (collector electrodes) arranged as concentric cylinders with 2.3 cm of internal radius. The transducer uses a High-Voltage-DC source (11 kV) to ionize the air in the corona electrode surroundings and a superimposed AC signal (100 Vrms) to modulate the plasma temperature and the ion velocity. In this arrangement the sound wave is generated by temperature changes in the corona electrode surrondings and by ion-neutral momentum transfer in the gap region [16]. The cylindrical directivity pattern of the transducer was checked using gating techniques [17]. This device was placed at the center of the cavity as displayed in Fig. 1. The dimensions of the cavity were chosen in order to lie within the region where the acoustic transducer behaves more like an ideal cylindrical source, for the frequency range used in the experiment. This means that the cavity was limited both in the radial direction to the region where the decay of the sound intensity follows an inverse distance law (<25 cm), and in the vertical direction to the region where the sound intensity is relatively constant (5 cm above and below the center of the transducer).

Measurements were carried out by inserting a microphone (Brüel & kJær type 4133) through holes made on the top plate in nine different positions, as displayed in Fig. 1a. The signal from the microphone was passed through a custom made impedance converter, a near-zero noise pre-amplifier (Sinnewald Research & Development), and then digitized using a computer sound card (M-Audio Audiophile 2496).

We employed two kinds of signals for the source: (a) narrow-band filtered white noise, and (b) exponential sweeps. The first type of signal was used in order to obtain the steady state intensity response of the cavity. The bandwidth of the filters was 500 Hz and the central frequencies ranged from 2 to 12 kHz with steps of 250 Hz. The frequency range was restricted to the region where the response of the transducer was flat along its vertical direction. For each central frequency the signal consisted of 20 repetitions of 100 ms of filtered noise bursts separated by 100 ms of silence. Filtered noise was Tukey windowed ($\alpha = 0.05$) to eliminate filter ringing. The recordings were also bandpass-filtered to reduce ambient noise and the sound intensity was averaged over repetitions. On the other hand, the exponential sweeps were employed in order to obtain the impulse response (IR) of the cavity [18]. The sweeps covered the range from 1 to 30 kHz in 30 s. The measurements were made under two conditions: (a) sonic crystal cavity, as displayed in Fig. 1, and (b) the same system with the aluminum cylinders removed and the holes covered by rubber as a reference for the previous condition.

In Fig. 2 we display a band diagram of the sonic crystal studied experimentally obtained using the plane wave expansion method. The first full band gap takes place between 5.5 and 6.5 kHz approximately (gray area). There are no other full band gaps under 20 kHz, but there are partial band gaps (transmission forbidden in ΓX direction) occurring around 4, 9, 11 and 17 kHz.

In order to compare the experimental results against a theoretical prediction we employed multiple scattering theory MST [19] and a resampling method as follows: (a) we computed the sound pressure as a function of frequency for a two-dimensional cavity inside a sonic crystal at the same receiver positions as in the experiment, from 2 to 12 kHz with a resolution of 1 Hz, (b) to emulate the response of a narrow-band filtered noise burst we first selected a fixed number of frequencies belonging to the corresponding band, (c) we assigned a random phase to each selected pressure and added them up, obtaining a response for each receiver position, (d) we repeated steps (b) and (c) many times (resampling method) averaging the responses in order to obtain an approximating distribution of the response to a noise band. The spatial characteristics of the experimental sound source were further incorporated into the MST computation using an array of 16 radial dipoles at the same locations as the corona/collector pairs.

3. Results and discussion

We characterized the frequency response of the cavity using the intensity gain magnitude, defined as the ratio between the intensity measured in the sonic crystal cavity excited by the noise bands and the intensity of the same stimuli with the cylinders removed (reference condition), expressed in dB. In Fig. 3 we display the intensity gain of the cavity against the central frequency of the noise bands. The gray lines correspond to the values of this

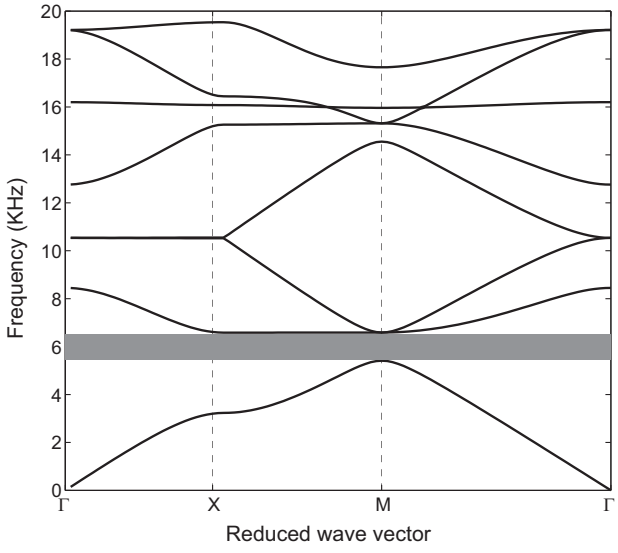

Fig. 2. Band structure of the sonic crystal used in the experiment obtained using the plane-wave method. The first full band-gap is shaded in gray.

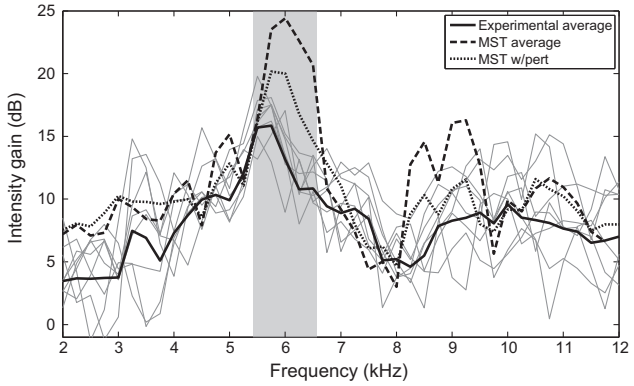

Fig. 3. Intensity gain (dB) of the sonic crystal cavity with respect to the sample with the sonic crystal removed (reference), against the central frequency of the noise bands. The gray lines correspond to the each of the measurement points depicted in Fig. 1, while the solid black line corresponds to their average value. The shaded region indicates the limits of the full band gap (BG) region. Within this region strong reinforcements up to 16 dB are observed. The Intensity gain obtained from MST calculations is displayed in dashed line. After a small perturbation of the positions of the cylinders (see text), the intensity gain obtained from MST calculation decreases (dotted line).

magnitude at each measuring point, while the averaged value is displayed in solid black line. A clearly noticeable increase in the intensity gain, with a peak value up to 16 dB, is observed along the frequency range of the full band gap (shaded area), for all measuring points. Comparing the results at different points also allows us to evaluate the spatial variability of the magnitudes. It is remarkable that the lowest variability in the intensity gain is obtained at the peak. This is consistent with the predictions of the previously reported model [14], where the lower spatial variability is observed for the full band-gap region.

The increase in the intensity gain within the full band-gap region is also observed for the results obtained from MST calculations (dashed line in Fig. 3). In this case the peak reaches 23.5 dB at 6 kHz. Two smaller peaks are also observed for the MST curve at 9 and 11 kHz, corresponding to the partial band-gap regions. The main differences between the experimental and theoretical results are the magnitude of the resonances (much higher for the MST calculation) and the presence of resonances for partial band-gap frequency regions. There are constructive limitations of the experimental setup that can explain these differences. While the MST calculations were performed for an ideal two-dimensional sonic crystal, the experimental cavity is inevitably three-dimensional, with additional losses, and with small deviations in the lattice positions of the cylinders. In order to test this last feature, we carried out an additional MST calculation after perturbing the lattice positions of the cylinders by a small amount (uncorrelated bivariate normal distribution with a standard deviation of 1 mm). The results for the intensity gain for this case with perturbation are displayed in Fig. 3 in black dotted line, compared to the experimental results (solid black line) and the results obtained from MST calculations without perturbation (dashed line). It is worth noting that the main effect of the perturbation on the intensity gain is a decrease in the magnitude of the highest peaks. Despite the remaining differences between the experimental and theoretical results, the only robust broadband resonance that persists, both for theoretical and experimental intensity gains, is that corresponding to the full band-gap region.

A quantitave measure of the losses can be obtained from the decay times of the cavity. We calculated these times as a function of frequency by applying the Schroeder integration method [20] to the obtained impulse responses of the cavity, filtered with the same filters as used for the noise bands, and estimating the time it takes the signal to drop by 60 dB (as in the standard reverberation time employed in room acoustics). Fig. 4 depicts the decay times inside the cavity for all measuring points (gray lines) along with their average across measuring points (solid black line). As a reference, the decay time of the sample with the cylinders removed is displayed in dashed black line. We also included the decay times calculated from the response of the cavity to the noise band stimuli using the same method as before after the extintion of the signal. (square symbols). As with the intensity gain, there is a distinct peak within the region of the total band gap, indicating that the energy decays at a slower rate. The peak finds its maximum value of 78 ms about the center of the band gap (6 kHz). In order to give some meaning to this decay time in terms of the cavity losses we can make use of an ergodic approximation (as in the derivation of the Sabine's law in room acoustics [21]) restricted to two dimensions and estimate the decay time (τ_{2D}) for a two-dimensional cavity of area A and perimeter P as [22]: $\tau_{2D} = \frac{\pi cA}{\alpha P}$, where α is a constant absorption coefficient, and c is the sound velocity. This approximation gives a value for the absorption coefficient of $\alpha = 0.0014$. Thus, as we anticipated, within the full band-gap region the sonic crystal walls act as strong reflectors ($R = 0.9986$), losing less than a 0.2% of the incident energy on each reflection. This absorption value, although small, could explain the remaining 5 dB difference between the intensity gain peaks obtained from the experiment and from the perturbed MST calculations (see Fig. 3).

We now turn on the possible origin of the broadband resonance. As it was previously theoretically predicted [14] and derived above from our measurements, for frequencies within the full band-gap region the reflection coefficient of the sonic-crystal walls can be considered close to unity for all angles of incidence and the energy is trapped inside the cavity for a relatively long period of time. In contrast, for frequencies belonging to the partial band gap regions, the reflection coefficient is close to unity only for certain angles of incidence. As an example of this last case, from the band diagram displayed in Fig. 2 it is apparent that at the partial band gaps around 4 and 9 kHz the forbidden propagation direction inside the crystal, and consequently the total reflection at the boundary, corresponds to normal incidence (direction ΓX). Hence, for the ideal two-dimensional case, within the full band-gap region one can expect the appearance of many modal resonances, without restrictions in the orientation of the wavevectors, as long as the dimension of the cavity is much larger than their corresponding wavelengths. Instead, for the partial band gap region, where total

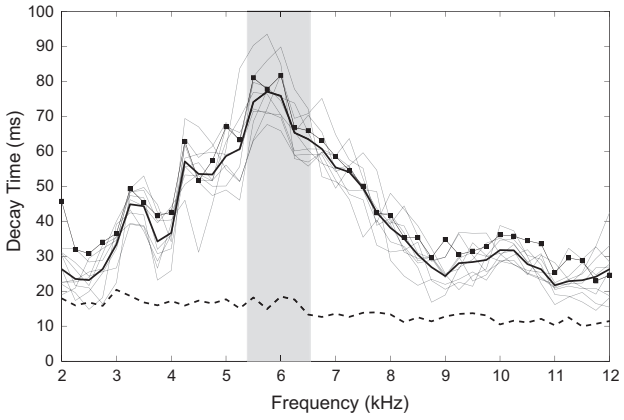

Fig. 4. Average decay time of the sound inside the sonic crystal cavity against frequency obtained from the impulse response (solid black line) and from the noise bands (square symbols), compared to the average decay time sample with the sonic crystal removed (dashed line). Gray lines correspond to the decay time at each measurement point.

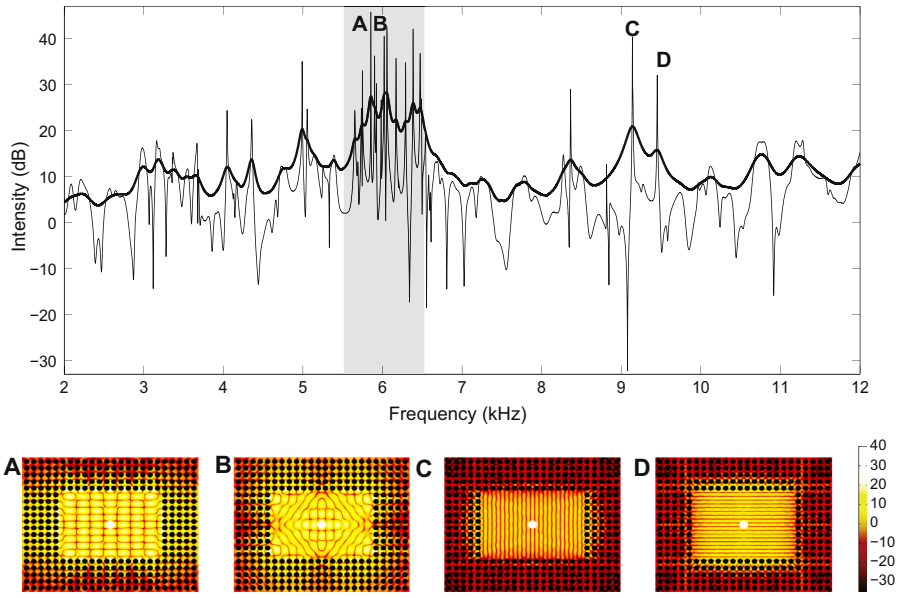

Fig. 5. Transfer function (sound pressure level as a function of frequency) at a representative measurement point for the simulated two-dimensional sonic crystal cavity using MST calculations (thin solid line), and the same curve after performing a convolution with lorentzian-shape peaks with frequency-dependent bandwidths derived from the decay times displayed in Fig. 4 (thick solid line). The insets A–D display the sound pressure level field of the cavity and the sonic crystal for some selected modal resonances indicated in the transfer function plot.

reflection is only attained for normal incidence, one can still expect the appearance of modes, but only restricted to a single axial direction.

These modal resonances can be observed in the frequency response of the idealized two-dimensional cavity obtained from MST calculations. In Fig. 5 (thin solid line) we display the transfer function for one receptor position calculated from MST. The peaks in the transfer function correspond to modal resonances, and four examples of the MST-computed sound fields are displayed beneath the graph. A higher density of modes can be appreciated within the full band-gap region (indicated by the shaded region), including axial, tangential (as the inset A in Fig. 5) and other exotic modal resonances that are peculiar to the sonic crystal cavity (as the inset B in Fig. 5). In contrast, for the partial band-gap (with total reflection only for normal incidence) the modes are sparse and correspond only to axial modes of the cavity, as shown in the insets C and D of Fig. 5. Also, note that there are narrow frequency regions where modal resonances are absent (for example around 4.5 kHz and 7.5 kHz) and the transfer function finds local minima. Thus, it is expected that the intensity gain obtained from MST calculations using noise bands near these regions also displays local minima (see Fig. 3). To further illustrate this point, a video component displaying an animation of the sound pressure level of the sonic crystal cavity as a function of frequency is available in the electronic version of this manuscript.

Perturbations of the lattice and losses due both to the finite size of the cylinders and to the divergence of the sound beam (among other constructive limitations) lead to an inevitable broadening of the modal resonances, and eventually to the overlap of neighboring peaks in the transfer function within the full band-gap region, giving rise to a single broadband resonance. In order to quantify this overlap, we employed the decay times obtained from the experiment to predict the broadening of the modal resonances and derive a transfer function more realistic than the one derived from MST calculations. The half-power bandwith B of the resonances can be obtained from the decay times τ simply using [21]: $B = 2.19/\tau$. These resonant peaks are much broader that the ones obtained from the MST calculations. Therefore, we made a convolution of these peaks (with the bandwith computed from the experimental decay time nearest in frequency) with the MST transfer function and obtained a smoother curve, that is displayed as thick solid line in Fig. 5. In this last curve we can see how, due to the widening of the peaks, the resonances within the full bad-gap become fused in a single broadband-like resonance.

4. Conclusions

This study reports an experimental validation of the existence of a broadband resonance in a rectangular cavity inside a sonic crystal. Unlike previous works, the dimensions of the free space surrounded by the sonic crystal walls are large compared both to the radii of the cylinders and the lattice parameter. This resonance is associated with the total reflection of the acoustical waves for all angles of incidence that occurs within the range of frequencies for which the sonic crystal displays a full band-gap. A comparison with a model of the cavity shows a good quantitative agreement for the frequency range of the resonance. Also, we discussed a possible origin of the broadaband resonance from the overlapping of the modal resonances present in the full band-gap frequency region, although further research is required to confirm this hypothesis.

Given that the band-gap range is determined by the structure of the sonic crystal, and not by the particular dimensions of the cavity, modifications of the diameters of the cylinders along with manipulations of the lattice constant would allow these systems to be tuned both to establish the central frequency of a resonant band as well as its corresponding bandwidth. Together with the relatively easy and inexpensive manufacturing of sonic crystals this feature could lead to potential applications of these systems in acoustic circuit design and smart acoustic materials.

Acknowledgments

The authors acknowledge the support of Guillermo Santiago from GLOMAE and Daniel Sinnewald from LACEAC, and Ramiro

Vergara from UNQ for useful discussions. This work was partially funded by CONICET and UNQ.

Appendix A. Supplementary material

Supplementary data associated with this article can be found, in the online version, at http://dx.doi.org/10.1016/j.apacoust.2015.10.022.

References

[1] Sigalas M. Elastic wave band gaps and defect states in two-dimensional composites. J Acoust Soc Am 1997;101(3):1256–61. http://dx.doi.org/10.1121/1.418156.
[2] Feng L, Liu X-P, Chen Y-B, Huang Z-P, Mao Y-W, Chen Y-F, Zi J, Zhu Y-Y. Negative refraction of acoustic waves in two-dimensional sonic crystals. Phys Rev B 2005;72(3):1–4. http://dx.doi.org/10.1103/PhysRevB.72.033108.
[3] Lu M-H, Zhang C, Feng L, Zhao J, Chen Y-F, Mao Y-W, Zi J, Zhu Y-Y, Zhu S-N, Ming N-B. Negative birefraction of acoustic waves in a sonic crystal. Nature Mater 2007(10):744–8. http://dx.doi.org/10.1038/nmat1987.
[4] Håkansson A, Sanchez-Dehesa J, Sanchis L. Acoustic lens design by genetic algorithms. Phys Rev B 2004;70(21):1–9. http://dx.doi.org/10.1103/PhysRevB.70.214302.
[5] Sanchez-Dehesa J, Garcia-Chocano VM, Torrent D, Cervera F, Cabrera S, Simon F. Noise control by sonic crystal barriers made of recycled materials. J Acoust Soc Am 2011;129(3):1173. http://dx.doi.org/10.1121/1.3531815.
[6] Li X-F, Ni X, Feng L, Lu M-H, He C, Chen Y-F. Tunable unidirectional sound propagation through a sonic-crystal-based acoustic diode. Phys Rev Lett 2011;106(8):1–4. http://dx.doi.org/10.1103/PhysRevLett.106.084301.
[7] Cicek A, Adem Kaya O, Ulug B. Refraction-type sonic crystal junction diode. Appl Phys Lett 2012;100(11):111905. http://dx.doi.org/10.1063/1.3694020.
[8] Li B, Guan J-J, Deng K, Zhao H. Splitting of self-collimated beams in two-dimensional sonic crystals. J Appl Phys 2012;112(12):124514. http://dx.doi.org/10.1063/1.4770471.
[9] Alagoz S, Alagoz BB. Sonic crystal acoustic switch device. J Acoust Soc Am 2013;133(6):EL485. http://dx.doi.org/10.1121/1.4807306.
[10] Sanchis L, Cervera F, Sanchez-Dehesa J, Sanchez-Perez JV, Rubio C, Martinez-Sala R. Reflectance properties of two-dimensional sonic band-gap crystals. J Acoust Soc Am 2001;109(6):2598. http://dx.doi.org/10.1121/1.1369784.
[11] Sanchis L, Håkansson A, Cervera F, Sanchez-Dehesa J. Acoustic interferometers based on two-dimensional arrays of rigid cylinders in air. Phys Rev B 2003;67(3):035422. http://dx.doi.org/10.1103/PhysRevB.67.035422.
[12] Wu L-Y, Chen L-W. Enhancing transmission efficiency of bending waveguide based on graded sonic crystals using antireflection structures. Appl Phys A 2012;107(3):743–8. http://dx.doi.org/10.1007/s00339-012-6800-2.
[13] Wang Y, Deng K, Xu S, Qiu C, Yang H, Liu Z. Applications of antireflection coatings in sonic crystal-based acoustic devices. Phys Lett A 2011;375(10):1348–51. http://dx.doi.org/10.1016/j.physleta.2011.02.004.
[14] Spiousas I, Eguia MC. Directional impulse response of a large cavity inside a sonic crystal. J Acoust Soc Am 2012;132(4):2842–51. http://dx.doi.org/10.1121/1.4744946.
[15] Wu L-Y, Chen L-W, Liu C-M. Acoustic energy harvesting using resonant cavity of a sonic crystal. Appl Phys Lett 2009;95(1):013506. http://dx.doi.org/10.1063/1.3176019.
[16] Bequin P, Castor K, Herzog P, Montembault V. Modeling plasma loudspeakers. J Acoust Soc Am 2007;121(4):1960. http://dx.doi.org/10.1121/1.2697201.
[17] Moller H, Carsten T. Electroacoustic free-field measurements in ordinary rooms using gating techniques. Audio Engineering Society Convention 108 52. <http://www.aes.org/e-lib/browse.cfm?elib=2370>.
[18] Farina A. Simultaneous measurement of impulse response and distortion with a swept-sine technique. Audio Engineering Society Convention 108. <http://www.aes.org/e-lib/browse.cfm?elib=10211>.
[19] Kafesaki M, Economou EN. Multiple-scattering theory for three-dimensional periodic acoustic composites. Phys Rev B 1999;60:11993–2001. http://dx.doi.org/10.1103/PhysRevB.60.11993.
[20] Schroeder M. New method of measuring reverberation time. J Acoust Soc Am 1965;37(3):409–12. http://dx.doi.org/10.1121/1.1909343.
[21] Kuttruff H. Room acoustics. Fifth ed. New York: Taylor & Francis; 2009.
[22] Legrand O, Sornette D. First return, transient chaos, and decay in chaotic systems. Phys Rev Lett 1991;66. http://dx.doi.org/10.1103/PhysRevLett.66.2172. 2172–2172.